A28 Vol. 36, No. 2 / February 2019 / Journal of the Optical Society of America B Research Article

Journal of the Optical Society of America B OPTICAL PHYSICS

Focusability of laser pulses at petawatt transport intensities in thin-film compression

D. M. Farinella,[1,*] J. Wheeler,[2] A. E. Hussein,[3] J. Nees,[3] M. Stanfield,[1] N. Beier,[1] Y. Ma,[3] G. Cojocaru,[4] R. Ungureanu,[4] M. Pittman,[5] J. Demailly,[5] E. Baynard,[5] R. Fabbri,[6] M. Masruri,[6] R. Secareanu,[6] A. Naziru,[6] R. Dabu,[6] A. Maksimchuk,[3] K. Krushelnick,[3] D. Ros,[5] G. Mourou,[2] T. Tajima,[1] and F. Dollar[1]

[1]Department of Physics and Astronomy, University of California, Irvine, California 92697, USA
[2]DER-IZEST, Ecole Polytechnique, 91128 Palaiseau Cedex, France
[3]Center for Ultrafast Optical Science, University of Michigan, Ann Arbor, Michigan 48109, USA
[4]Center for Advanced Laser Technologies (CETAL) - National Institute for Laser, Plasma and Radiation Physics (INFLPR), 409 Atomistilor, Magurele 077125, Romania
[5]LASERIX (Université Paris-Sud - LUMAT), Orsay, France
[6]Extreme Light Infrastructure Nuclear Physics (ELI-NP) National Institute for R&D in Physics and Nuclear Engineering (IFIN-HH), Magurele-Bucharest, Romania
*Corresponding author: dfarinel@uci.edu

Received 18 September 2018; revised 3 November 2018; accepted 5 November 2018; posted 5 November 2018 (Doc. ID 346015); published 4 December 2018

Thin-film compression (TFC) and the focusability of high-power laser pulses after self-phase modulation in thin films at transport intensities (~1 TW/cm^2) for petawatt laser systems is demonstrated. High-energy (~296 mJ) laser pulses are compressed from ~55 fs to ~31 fs. Additionally, the focusability of high-power (~45–55 TW) flat-top laser pulses after spectral broadening in thin films is found to be largely maintained, showing only modest decreases in the energy contained in the central part of the focal spot. In light of these findings, TFC offers a method for moving toward single-cycle pulse durations at significantly higher energies than those found at present, and if beam instabilities can be mitigated, maybe even higher intensities.

https://doi.org/10.1364/JOSAB.36.000A28

1. INTRODUCTION

Next-generation laser driven accelerators and high field science [1–4] require laser technology with shorter pulse durations and higher peak power than is currently available. Much progress has been made in the past few decades, most notably with the introduction of chirped pulse amplification (CPA) [5] enabling ultrashort laser systems to reach peak power levels currently at the petawatt level [6]. Facilities across the world are working to increase the peak power of their laser systems by developing higher energy lasers in order to reach 10 PW at the extreme light infrastructure (ELI) [7] or even 100 PW at the Station of Extreme Light (SEL) [8] in Shanghai. Meanwhile, the pulse length–intensity conjecture [9] suggests that the compression of laser pulses to an ultimate limit perhaps provides an alternative path to high intensities.

To achieve pulse compression of a transform-limited laser pulse, there are two requirements: (1) its bandwidth must be broadened, and (2) the broadened bandwidth must be brought into phase. Optical pulse compression techniques [10–17] achieve this by making use of the optical Kerr effect $n(r,t) = n_0 + n_2 I(r,t)$, where n_0 is the index of refraction, n_2 is the nonlinear index of refraction, and $I(r,t)$ is the intensity. The temporal intensity envelope causes a nonlinear phase shift called self-phase-modulation (SPM) [18,19], leaving the pulse envelope unchanged and therefore resulting in a broadened spectrum. In the case of a Gaussian temporal envelope, SPM causes a linear frequency chirp $\omega_{\text{inst}}(t) = \omega_0 - k_0 n_2 z dI(t)/dt$ in the central region of the pulse where the temporal intensity envelope is approximately quadratic. Here $\omega_{\text{inst}}(t)$ is the instantaneous frequency, k_0 is the central wavenumber, and z is the thickness of the nonlinear material. This linear chirp can then be removed by chirped mirrors, bringing the spectral components into phase, and constructing a shorter pulse than before. As seen above, the spatial dependence of the intensity profile can also affect the index of refraction, which can result in whole-beam self-focusing or small-scale filamentation, depending on factors including mode type and peak power, which will be further discussed in Section 4.

To scale pulse compression to petawatt laser systems, a technique called "thin-film compression" (TFC) has been suggested by Mourou *et al.* [20] following the work of Mevel *et al.* [21]

and Mironov *et al.* [22]. This technique overcomes energy limitations of conventional pulse compression techniques using gas-filled capillaries (∼1 mJ) imposed by ionization and energy losses due to mode coupling with the capillary [23] and has recently been simulated [24] demonstrated using petawatt beams [25]. Using intense pulses (∼1 TW/cm^2) and thin plastic films, a flat-top beam from a high-energy laser would induce uniform SPM across the beam profile with no restriction on aperture size. The initial TFC proposal suggested the use of plastic films, but here we test uncoated fused silica (FS) wafers, which have a lower Kerr response than plastic. For the same initial pulse, this lower Kerr response can be offset by increasing the amount of material involved in the interaction as the extent of spectral broadening is directly proportional to these values. At the same time, minimizing the amount of material introduced helps to avoid small-scale self-focusing within the bulk, and therefore 0.5 mm thick wafers are considered as they might prove useful in cases requiring higher damage thresholds than what plastics can provide. Further, when the FS wafer is oriented at Brewster's angle, reflective losses can be minimized, making this process very energy efficient. With chirped mirror reflectivity of ≥ 99.5%, the largest losses from this technique are expected to arise from surface reflections, material absorption, and small-scale filamentation arising from the pulse interaction with the thin film.

To reach the highest intensities for experiments, intense pulses are focused to focal spots with diameters on the order of the wavelength. It is therefore imperative that the wavefront quality be maintained in the pulse compression technique used. The unguided propagation of intense pulses in nonlinear materials can lead to wavefront imperfections [26–29] that may impair the focusability of intense pulses. In lower-intensity pulse compression techniques it is common to use waveguiding structures to maintain wavefront quality.

In this paper, we present experimental results of TFC of intense pulses far beyond the energy threshold for conventional techniques (∼296 mJ). Further, to determine the significance of the accumulation of wavefront errors as the laser power is increased toward the petawatt level, we present experimental results of the focusability of spectrally broadened intense pulses after propagation in thin FS wafers at even higher power. Two different short-pulse laser systems are used to carry out this study: the HERCULES laser [30] located at the the Center for Ultrafast Optical Science (CUOS) at the University of Michigan–Ann Arbor, and the LASERIX facility located at the Université Paris-Sud in Orsay, France.

In Section 2, high-energy TFC of intense pulses is demonstrated at LASERIX after a brief description of the diagnostics used to obtain the data. Section 3 investigates the effect on the focusability of larger-scale, high-intensity pulses after SPM in a thin FS wafer at the HERCULES facility. Finally, in Section 4, the outlook for pulse compression using thin materials is discussed in the context of the experimental findings.

2. THIN-FILM COMPRESSION

The general layout of the LASERIX experiment can be seen in Fig. 1. Intense pulses (∼1.9 TW/cm^2) are first spectrally broadened in a 0.5 mm FS wafer in a vacuum at near normal

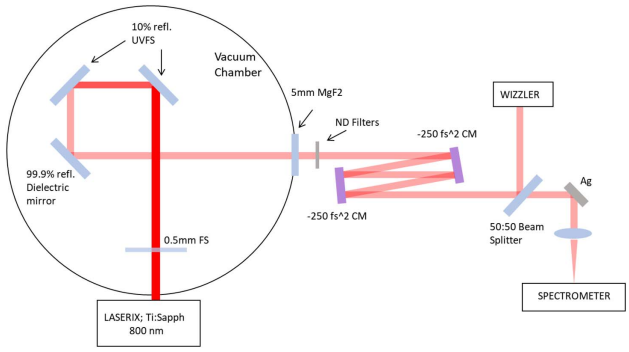

Fig. 1. Schematic of the LASERIX experiment showing the attenuation scheme, phase compensation, and spectral and temporal diagnostics.

incidence. The intensity is estimated based on the measured laser pulse energy ∼296 mJ, taken together with a measured pulse duration of 50 fs. The *s*-polarized beam is then attenuated by a factor of ∼100 immediately after the interaction by reflections from 2× UV-grade fused silica (UVFS) windows with a frosted back to prevent back-reflections. After attenuation, the pulses travel through the MgF2 vacuum window with low enough intensity such that no nonlinear effects are expected or observed (B ∼0.04). The chirped mirrors are placed outside of the vacuum chamber to permit easy adjustment and after attenuation as a precaution against damage. Being constructed of a dielectric stack of thin films, these optics are expected to be robust to intensities of ∼1 TW/cm^2, although detailed damage studies will be an important topic for future studies. The pulses then take 4× bounces on chirped mirrors compensating for −1000 fs^2 of group delay dispersion (GDD). As shown in Fig. 1, a fiber spectrometer is used to measure the fundamental laser spectrum. A lens is used to focus the laser onto a ceramic diffuser to couple the light into the fiber. The pulse duration of laser pulses with the 0.5 mm FS wafer in the beam (compressed) and without (initial) are measured by a Wizzler (self-referenced spectral interferometry, SRSI).

Shown in Fig. 2(a) is the initial (blue) and broadened (red) spectrum measured by the fiber spectrometer. The broadened spectrum is obtained by manipulating the compressor grating separation with the FS wafer in the beam to find the broadest spectrum. The wafer is removed from the beam to obtain a measurement of the initial spectrum. The FWHM of the

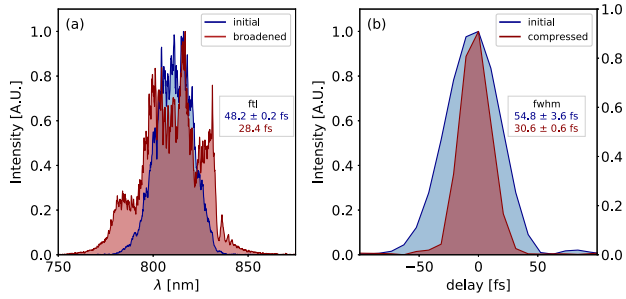

Fig. 2. (a) Laser spectrum and (b) pulse duration with (red) and without (blue) the 0.5 mm FS wafers in the beam. The spectral broadening (a) and pulse compression (b) shown here are measured by the fiber spectrometer and Wizzler (SRSI), respectively.

Fourier transform limit (FTL) of the spectrum before and after spectral broadening is found to be 48.2 ± 0.2 fs and 28.4 fs, respectively, as noted in Fig. 2(a). The FTL presented here represents an average of 5 spectrometer measurements for the initial pulse and a single spectrometer measurement for the broadened spectrum, where the uncertainty represents the standard deviation in these measurements. The extent of spectral broadening in this case is very close to the expected value from SPM theory. Nonlinear simulations using the open-source Python software package pyNLO [31] were carried out, propagating a pulse with the experimentally measured parameters and zero phase through 0.5 mm FS. This package solves the nonlinear Schrödinger equation accounting for group velocity dispersion, self-phase modulation, self-steepening, and Raman effects. The resulting FTL after propagation through the 0.5 mm FS wafer was ∼28 fs, implying that the experimental spectral broadening was very close to optimized. The FTL of the simulated spectrum was calculated in the same way as the FTL of the experimental data by Fourier transforming all of the signal above 1% of the maximum intensity.

Similarly Fig. 2(b) shows the initial (blue) and compressed (red) pulse duration as measured by SRSI. The FWHM duration of the initial and compressed pulse is found to be 54.8 fs ± 3.6 fs and 30.6 ± 0.6 fs, respectively. The FWHM presented here represents an average of five shots in each case, where again the uncertainty represents the standard deviation of these measurements. It is noted here that the temporal measurements in this section correspond to an irised sample of the beam profile, which is indicative of the full beam profile. The initial pulse duration is slightly longer than the FTL as expected due to the chirp incurred by the chirped mirrors. Once the FS wafer is introduced to the beam, the spectrum is broadened, and the spectral components are brought into phase, constructing a pulse very near the FTL.

3. FOCUSABILITY OF HIGH-POWER SPECTRALLY BROADENED PULSES

The general experimental layout of the HERCULES experiment can be found in Fig. 3. Intense pulses (∼0.6–0.7 TW/cm^2) are spectrally broadened in a 0.5 mm FS wafer in a vacuum as in the last section. The HERCULES laser produces pulses with durations of down to 30 fs [30]. The estimation of intensity was made based on diode energy measurements of ∼2.2–2.6 J combined with the FTL of the initial spectrum (∼48 fs) and serves as an upper bound to the intensity in this particular

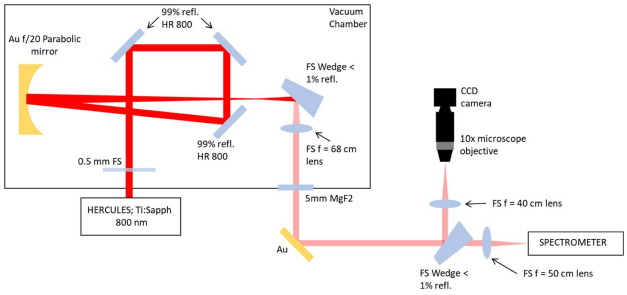

Fig. 3. Schematic of the HERCULES experiment showing the attenuation scheme, focal spot imaging, and spectral diagnostics.

experimental run. After creating a focus with an $f/20$ parabolic mirror, the p-polarized beam is attenuated by >100 times with a UVFS wedge at near 45 deg. This allows the beam to be re-collimated and exit the chamber through the MgF2 window with negligible nonlinearity. The beam is further attenuated after reflection from a wedge, and the focus is re-imaged onto a CCD camera, where the pixel size is calibrated to the focal spot size of the parabola. The beam transmitted through the wedge is focused into a spectrometer to monitor the pulse spectrum. Unlike the LASERIX setup, experimental constraints at HERCULES require that the FS wafer cannot be removed *in situ*, so the grating separation was decreased (adding positive chirp to the pulse) to minimize spectral broadening in order to determine the unbroadened laser spectrum. Negatively chirped pulses are not included here due the observed effect of spectral narrowing through SPM in fused silica [32].

The focusability of the initial and spectrally broadened intense pulses are investigated by measuring how the focal spot changes with and without spectral broadening. Using this technique, one can isolate the effect of the nonlinearity on the focal spot without the complication of adding or removing optics. In this way, the changes in the focal spot can be interpreted as changes due to the nonlinear interaction.

Plotted in Fig. 4(a) is the average horizontal line-out of the focal spot intensity distribution for the spectrally broadened (red) and initial (blue) pulses. Here the shading represents the standard deviation of the profiles of three initial shots and four broadened shots. Figures 4(b) and 4(c) show the measured focal spots for the initial and spectrally broadened pulses, respectively. The dashed horizontal line overlay corresponds to the location of the line-outs shown on (a). In Fig. 4(a), the line-outs from the peak counts are superimposed in order to highlight the redistribution of the intensity at the focal plane by the introduction of the nonlinear interaction.

With increasing intensity, the nonlinear response within the FS wafer causes the HERCULES spectrum to broaden to a point capable of supporting a FTL pulse at 87.5% of its initial FWHM. As seen in the LASERIX experiment, laser pulses broadened in this way are compressible through the use of chirped mirrors to near the FTL, and this suggests that the HERCULES pulses could be compressed to 87.5% of their initial duration if the appropriate dispersion compensation was applied. For the larger-scale beam profile, the pattern of the focal spot is maintained while there is some energy

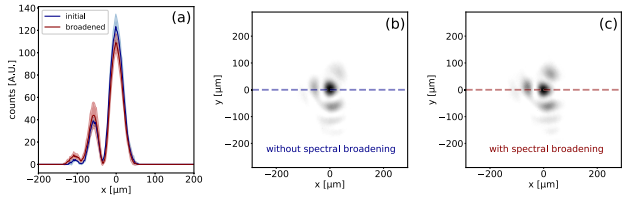

Fig. 4. Average horizontal focal spot line-out at the max signal value (a) for initial (blue) and spectrally broadened (red) pulses and sample focal spots of the (b) initial and (c) broadened pulses. The shading in (a) represents the standard deviation of all broadened (light red) and initial (light blue) focal spot line-outs. The overlays of the line-out location on the initial focal spot and the spot after spectral broadening are shown in (b) and (c), respectively.

redistribution away from the central main portion of the focus due to the SPM. Quantitatively, the energy contained in the HERCULES central spot (within the first minima) is seen to change from 49% ± 3% to 38% ± 4% with the introduction of the nonlinear spectral broadening. Further, the peak counts are seen to drop from 123 ± 14 to 109 ± 10, which represents a decrease in peak fluence of ∼88.6%. Here the percent energy contained and peak counts represent the average of three initial shots and four broadened shots, respectively, and the uncertainty represents the standard deviation among these shots. The change in average energy contained in the central spot may be due to filamentation, which is an expected challenge in high-energy systems, which is discussed in more detail in the following section. The decrease in average peak signal coupled with the decrease in average potential pulse duration of roughly the same percent make it difficult to determine if the peak intensity could be increased through pulse compression based on this data due to the variability in shot-to-shot pulse energy at HERCULES. On the other hand, this data suggests that high-power laser pulses such as those of HERCULES could be compressed and focused to the approximately the same focal intensities, providing a route to the relativistic single-cycle regime.

4. DISCUSSION

High-power laser pulses such as those of HERCULES and LASERIX typically have flat-top modes due to amplification in multi-pass amplifiers. In a multi-pass amplifier, gain saturation is bypassed by taking different geometrical paths through the gain medium. This maximizes the extraction of energy from the gain medium [33]. When the peak power of the pulse exceeds the critical power $P_{cr} = \pi(0.61)^2\lambda_0^2/(8n_0n_2)$ [34] (∼2.6 MW for fused silica at 800 nm), the laser mode and diameter play an important role in how the focusability is affected through the nonlinear Kerr effect. The critical power is the threshold at which whole-beam self-focusing of a Gaussian beam due to the Kerr effect just compensates for the beam spreading due to diffraction [35]. For intense pulses with super-Gaussian modes, instead of whole-beam self-focusing, beam collapse is slightly different and tends to be initiated by noise in the beam profile [36]. These pulses tend to be susceptible to multi-filamentation through the modulational instability [27] where a beam with $P \gg P_{cr}$ is understood to break up into multiple filaments during propagation through a nonlinear medium of sufficient length, each with power of order $\sim P_{cr}$ [37].

In the context of spectral broadening for pulse compression, these mode effects are conventionally avoided by inducing SPM in gas-filled hollow-core capillaries, which only allow for the propagation of the fundamental mode at sufficient length [15]. However, the energy of intense pulses spectrally broadened in this guided process are limited to the order of ∼1 mJ, where self-focusing and ionization of the gas near the entrance of the fiber degrades the coupling to the fiber and therefore broadening due to SPM [23].

TFC pushes past these barriers by using thin nonlinear material for SPM (as in recent results using a similar technique at energies up to 21 mJ [38,39]) of flat-top intense pulses and re-compression with chirped mirrors as demonstrated by the pulse compression of ∼296 mJ pulses in the LASERIX experiment. Further, spatially filtering the beam before each nonlinear interaction as suggested in TFC [40], or taking advantage of the self-filtering based on free-space propagation [41–43], allows for the minimization of filamentation and removal of noise before the modulational instability is allowed to grow [37,44]. In the HERCULES experiment, the focal spot was maintained without the necessity of spatial filtering. It is expected that the focal spot quality of the spectrally broadened pulse would only improve with the introduction of spatial filtering before the nonlinear interaction. Quantifying the improvement in focal spot quality with the implementation of spatial filtering before the nonlinear interaction is very important and warrants investigation in future studies but is beyond the scope of this paper.

The experimental demonstration of pulse compression from ∼55 fs to ∼31 fs using thin FS wafers in a single stage is applicable for any beam mode that has a uniform intensity or flat-top profile. Additionally, as suggested in [40], a second stage could be utilized after spatial filtering to further decrease pulse duration towards the single-cycle regime.

5. CONCLUSION

TFC of ∼296 mJ intense pulses in 0.5 mm FS wafers from ∼55 fs to ∼31 fs has been demonstrated. Further, the focusability of high-power (45–55 TW) spectrally broadened intense pulses after nonlinear interaction in FS wafers has been investigated. After spectral broadening in FS wafers, the ability to create a well-defined focal spot is maintained with a modest decrease in energy contained in the central portion of the focal spot. These results suggest that multi-stage TFC using thin wafers may present a practical route to relativistic single-cycle laser pulses. Further, if modulational instabilities can be suppressed by spatially filtering before the nonlinear spectral broadening, TFC may even increase the peak intensity, pushing the limits on high field science.

Funding. National Science Foundation (NSF) STROBE (DMR 1548924); Norman Rostoker Fund; Alfred P. Sloan Foundation; Extreme Light Infrastructure - Nuclear Physics (ELI-NP) - Phase II; Laserlab-Europe (EU-H2020 654148); European Regional Development Fund (ERDF) through the Competitiveness Operational Programme "Investing in Sustainable Development" (1/07.07.2016, COP ID 1334).

Acknowledgment. The authors gratefully thank Sergey Mironov and Efim Khazanov for insightful discussions.

REFERENCES

1. T. Tajima and J. Dawson, "Laser electron accelerator," Phys. Rev. Lett. **43**, 267–270 (1979).
2. M. Zhou, X. Yan, G. Mourou, J. Wheeler, J. Bin, J. Schreiber, and T. Tajima, "Proton acceleration by single-cycle laser pulses offers a novel monoenergetic and stable operating regime," Phys. Plasmas **23**, 043112 (2016).
3. T. Tajima, "Laser acceleration in novel media," Eur. Phys. J. Spec. Top. **223**, 1037–1044 (2014).

4. G. Mourou and T. Tajima, eds., *Zetta-Exawatt Science and Technology*, vol. **223** of European Physical Journal Special Topics (Springer, 2014).
5. D. Strickland and G. Mourou, "Compression of amplified chirped optical pulses," Opt. Commun. **56**, 219–221 (1985).
6. M. D. Perry, D. Pennington, B. C. Stuart, G. Tietbohl, J. A. Britten, C. Brown, S. Herman, B. Golick, M. Kartz, J. Miller, H. T. Powell, M. Vergino, and V. Yanovsky, "Petawatt laser pulses," Opt. Lett. **24**, 160–162 (1999).
7. "Extreme Light Infrastructure (ELI)," 2018, https://eli-laser.eu/.
8. "Station of Extreme Light (SEL)," 2018, https://indico.sinap.ac.cn/.
9. G. Mourou and T. Tajima, "More intense, shorter pulses," Science **331**, 41–42 (2011).
10. R. A. Fisher, P. L. Kelley, and T. K. Gustafson, "Subpicosecond pulse generation using the optical kerr effect," Appl. Phys. Lett. **14**, 140–143 (1969).
11. D. Grischkowsky and A. Balant, "Optical pulse compression based on enhanced frequency chirping," Appl. Phys. Lett. **41**, 1–3 (1982).
12. C. V. Shank, R. L. Fork, R. Yen, R. H. Stolen, and W. J. Tomlinson, "Compression of femtosecond optical pulses," Appl. Phys. Lett. **40**, 761–763 (1982).
13. B. Nikolaus and D. Grischkowsky, "12× pulse compression using optical fibers," Appl. Phys. Lett. **42**, 1–2 (1983).
14. W. H. Knox, R. L. Fork, M. C. Downer, R. H. Stolen, C. V. Shank, and J. A. Valdmanis, "Optical pulse compression to 8 fs at a 5-kHz repetition rate," Appl. Phys. Lett. **46**, 1120–1121 (1985).
15. M. Nisoli, S. De Silvestri, and O. Svelto, "Generation of high energy 10 fs pulses by a new pulse compression technique," Appl. Phys. Lett. **68**, 2793–2795 (1996).
16. M. Nisoli, S. De Silvestri, O. Svelto, R. Szipöcs, K. Ferencz, C. Spielmann, S. Sartania, and F. Krausz, "Compression of high-energy laser pulses below 5 fs," Opt. Lett. **22**, 522–524 (1997).
17. C. Rolland and P. B. Corkum, "Compression of high-power optical pulses," J. Opt. Soc. Am. B **5**, 641–647 (1988).
18. F. Shimizu, "Frequency broadening in liquids by a short light pulse," Phys. Rev. Lett. **19**, 1097–1100 (1967).
19. R. H. Stolen and C. Lin, "Self-phase-modulation in silica optical fibers," Phys. Rev. A **17**, 1448–1453 (1978).
20. G. Mourou, G. Cheriaux, and C. Raider, "Device for generating a short duration laser pulse," U.S. patent 20110299152A1 (July 31, 2009).
21. E. Mével, O. Tcherbakoff, F. Salin, and E. Constant, "Extracavity compression technique for high-energy femtosecond pulses," J. Opt. Soc. Am. B **20**, 105–108 (2003).
22. S. Mironov, V. Lozhkarev, V. Ginzburg, and E. Khazanov, "High-efficiency second-harmonic generation of superintense ultrashort laser pulses," Appl. Opt. **48**, 2051–2057 (2009).
23. S. Bohman, A. Suda, T. Kanai, S. Yamaguchi, and K. Midorikawa, "Generation of 5.0 fs, 5.0 mJ pulses at 1 kHz using hollow-fiber pulse compression," Opt. Lett. **35**, 1887–1889 (2010).
24. A. A. Voronin, A. M. Zheltikov, T. Ditmire, B. Rus, and G. Korn, "Subexawatt few-cycle lightwave generation via multipetawatt pulse compression," Opt. Commun. **291**, 299–303 (2013).
25. S. Y. Mironov, V. N. Ginzburg, I. V. Yakovlev, A. A. Kochetkov, A. A. Shaykin, E. A. Khazanov, and G. A. Mourou, "Using self-phase modulation for temporal compression of intense femtosecond laser pulses," Quantum Electron. **47**, 614–619 (2017).
26. P. L. Kelley, "Self-focusing of optical beams," Phys. Rev. Lett. **15**, 1005–1008 (1965).
27. V. I. Bespalov and V. I. Talanov, "Filamentary structure of light beams in nonlinear liquids," ZhETF Pisma Redaktsiiu **3**, 471–476 (1966).
28. A. A. Voronin and A. M. Zheltikov, "Pulse self-compression to single-cycle pulse widths a few decades above the self-focusing threshold," Phys. Rev. A **94**, 023824 (2016).
29. A. A. Voronin and A. M. Zheltikov, "Power-scalable subcycle pulses from laser filaments," Sci. Rep. **7**, 36263 (2017).
30. V. Yanovsky, V. Chvykov, G. Kalinchenko, P. Rousseau, T. Planchon, T. Matsuoka, A. Maksimchuk, J. Nees, G. Cheriaux, G. Mourou, and K. Krushelnick, "Ultra-high intensity-300-TW laser at 0.1 Hz repetition rate," Opt. Express **16**, 2109–2114 (2008).
31. "pyNLO: Nonlinear optics modeling for Python," 2015, https://pynlo.readthedocs.io/en/latest/index.html.
32. M. Oberthaler and R. A. Hopfel, "Special narrowing of ultrashort laser pulses by self phase modulation in optical fibers," Appl. Phys. Lett. **63**, 1017–1019 (1993).
33. W. H. Lowdermilk and J. E. Murray, "The multipass amplifier: theory and numerical analysis," J. Appl. Phys. **51**, 2436–2444 (1980).
34. R. W. Boyd, "Processes resulting from the intensity-dependent refractive index," in *Nonlinear Optics*, 3rd ed. (Academic, 2008), Chap. 7, pp. 329–390.
35. W. Koechner, "Laser amplifier," in *Solid-State Laser Engineering*, Springer Series in Optical Sciences (Springer, 2006), pp. 156–209.
36. A. J. Taylor, T. S. Clement, and G. Rodriguez, "Determination of n_2 by direct measurement of the optical phase," Opt. Lett. **21**, 1812–1814 (1996).
37. A. M. Rubenchik, S. K. Turitsyn, and M. P. Fedoruk, "Modulation instability in high power laser amplifiers," Opt. Express **18**, 1380–1388 (2010).
38. P. He, Y. Liu, K. Zhao, H. Teng, X. He, P. Huang, H. Huang, S. Zhong, Y. Jiang, S. Fang, X. Hou, and Z. Wei, "High-efficiency supercontinuum generation in solid thin plates at 0.1 TW level," Opt. Lett. **42**, 474–477 (2017).
39. V. Shumakova, P. Malevich, S. Ališauskas, A. Voronin, A. M. Zheltikov, D. Faccio, D. Kartashov, A. Baltuška, and A. Pugžlys, "Multi-millijoule few-cycle mid-infrared pulses through nonlinear self-compression in bulk," Nat. Commun. **7**, 12877 (2016).
40. G. Mourou, S. Mironov, E. Khazanov, and A. Sergeev, "Single cycle thin film compressor opening the door to zeptosecond-exawatt physics," Eur. Phys. J. Spec. Top. **223**, 1181–1188 (2014).
41. V. N. Ginzburg, A. A. Kochetkov, A. K. Potemkin, and E. A. Khazanov, "Suppression of small-scale self-focusing of high-power laser beams due to their self-filtration during propagation in free space," Quantum Electron. **48**, 325–331 (2018).
42. S. Mironov, V. Lozhkarev, G. Luchinin, A. Shaykin, and E. Khazanov, "Suppression of small-scale self-focusing of high-intensity femtosecond radiation," Appl. Phys. B **113**, 147–151 (2013).
43. S. Y. Mironov, V. V. Lozhkarev, V. N. Ginzburg, I. V. Yakovlev, G. Luchinin, A. Shaykin, E. A. Khazanov, A. Babin, E. Novikov, and S. Fadeev, "Second-harmonic generation of super powerful femtosecond pulses under strong influence of cubic nonlinearity," IEEE J. Sel. Top. Quantum Electron. **18**, 7–13 (2012).
44. J. T. Hunt, J. A. Glaze, W. W. Simmons, and P. A. Renard, "Suppression of self-focusing through low-pass spatial filtering and relay imaging," Appl. Opt. **17**, 2053–2057 (1978).